ASTRONOMY & ASTROPHYSICS
SUPPLEMENT SERIES

Astron. Astrophys. Suppl. Ser. **137**, 43–49 (1999)

OH and H_2O masers in 74 star-forming regions⋆

The FC89 database

J.R. Forster[1] **and J.L. Caswell**[2]

[1] University of California, Berkeley, Hat Creek Radio Observatory, 42231 Bidwell Road, Hat Creek, CA 96040, U.S.A.
[2] Australia Telescope National Facility, CSIRO, PO Box 76, Epping, NSW 2121, Australia

Received September 9, 1998; accepted February 8, 1999

Abstract. Positions and spectra of 1665 MHz OH and 23 235 MHz H_2O masers in 74 star-forming regions are presented. This supplement provides an electronic version of the complete VLA database of interstellar masers observed by Forster & Caswell (1989). The fields observed comprise the majority of known interstellar OH and H_2O maser associations at galactic longitudes observable from both hemispheres. The database will be useful for interpreting continuum and molecular line observations of these regions, for investigations of the relationship between the masers and their local environment, and for temporal and kinematical studies of the masers themselves.

Key words: masers — HII regions — stars: pre-main sequence — catalogs

1. Introduction

The spatial relationship of interstellar OH and H_2O maser associations was investigated by Forster & Caswell (1989) - hereafter FC89) using VLA observations of 74 fields in the inner galaxy. The main aim of FC89 was to determine whether OH and H_2O masers coincide, and where they lie with respect to their exciting stars. The fields observed are a large sample of OH and H_2O masers with angular separation $< 15''$ in the galactic longitude range 335° to 50° and contains most of the southern maser associations known in 1985.

Send offprint requests to: J.R. Forster

⋆ Full version of Table 3 is available in electronic form at the CDS via anonymous ftp to cdsarc.u-strasbg.fr (130.79.128.5) or via http://cdsweb.u-strabg.fr/Abstract.html, and full version of Fig. 1 is available at the http://www.edpsciences.com

Correspondence to: rforster@astron.berkeley.edu

The VLA data showed that most OH and H_2O masers occur in small groups with diameters $\lesssim 30$ Mpc (10^{17} cm, $\sim$ 6 000 AU), and that the two groups generally coincide within the combined measurement errors ($\sim 1''$ rms). A detailed correspondence of maser spots between the two species was not found however, and FC89 concluded that the OH and H_2O masers occur near a common energy source, but in physically distinct zones. When an H II region is present the masers were found to lie within $\sim$20 mpc of the peak of the continuum emission, but not coincident with it.

Another important result of the FC89 survey is that the fields often contain several spatially distinct maser groups, not just a single OH/H_2O maser association. Altogether, 111 separate maser sites were found in the 74 fields mapped, including 36 isolated H_2O masers and 22 isolated OH masers. No H II regions were found at the location of isolated H_2O masers, whereas four were found near isolated OH maser groups.

While the general properties of the sample as a whole were analyzed and discussed in FC89, the spectra and spatial distribution of the masers in each field were not given. We will henceforth refer to the complete VLA database of OH and H_2O masers, including spectra and spotmaps, as the FC89 database.

Subsets of the FC89 database have already been used by various authors to establish the connection between water masers and warm molecular cores (Codella et al. 1997), to compare the OH & H_2O maser positions with other maser species (e.g. Kraemer & Jackson 1995; Ellingsen et al. 1996), and to investigate the relationship of the masers to continuum sources (Carral et al. 1997). Works in progress which make use of the database include a deep search for continuum sources at maser sites (Forster & Caswell, in preparation), 3 mm molecular line observations toward isolated masers, and measurements of dust emission toward OH and H_2O masers.

In view of the number of requests for the VLA data we have decided to publish the FC89 database in electronic form so it will be easily accessible. We believe that it will be useful for finding the locations of dense cores in molecular clouds, in investigating the spatial and kinematical relation between the masers and their local environment, and in studies of the temporal evolution of masers in star-forming regions.

2. The FC89 database

The VLA observations and data reduction are discussed in FC89 and will not be repeated here. The pertinent parameters are summarized in Table 1.

Table 1. VLA observations

Parameter	OH	H_2O
Date of observation	1983 Dec	1984 June
Frequency	1665 MHz	22.235 GHz
Polarization	LCP or RCP	RCP
Total bandwidth	0.195 MHz	6.25 MHz
Velocity resolution	0.55 km s^{-1}	1.32 km s^{-1}
VLA configuration	A-B Hybrid	C-array
Integration time	8 min	8 min
Number of antennas	18	18
Data reduction package	MAD	AIPS
Typical beam size	$5\farcs5 \times 1\farcs5$	$2\farcs5 \times 1\farcs4$
Field size imaged	$32''$	$51''$
Total channels mapped	∼1500	∼2700
Absolute position error	∼$0\farcs5$ rms	∼$0\farcs5$ rms
Relative position error	< $0\farcs3$ rms	< $0\farcs3$ rms

The entire OH and H_2O maser database is presented in two tables and one figure. Table 2 contains a list of reference positions for each field observed. These are H_2O maser positions, with the exception of the eight instances where no H_2O maser was detected and the OH maser positions are used. Both B1950 and J2000 coordinates are given, along with the kinematical distance and the synthesized beams (major and minor axes and position angle of the restoring Gaussian). The near and far distances are both listed unless there is no ambiguity. If the ambiguity has not been resolved but one distance is preferred, the other is enclosed in parentheses. For the 23 GHz continuum detections and the sense of circular polarization used for the OH observations, Table 1 of FC89 should be consulted.

The source names used are the same as in FC89. These are derived from the galactic coordinates of the OH maser reference positions, and may differ slightly from the galactic coordinates of the H_2O masers listed in Table 2. There is one additional field in Table 2 which was not listed in FC89. 8.68–0.37 is an isolated OH maser approximately 1 arcmin from the OH/H_2O maser association 8.67–0.36. This specific OH maser site has been referred to in several publications (e.g. Caswell 1998) and has therefore been given a separate listing here. There are three other fields which contain maser sites with large separations (348.70–1.04, 12.22–0.12 and 23.01–0.41), but these are listed as single entries for consistency with FC89.

While a position for 19.61–0.13 is given in Table 2, this weak, isolated OH maser is not included in Table 3 or in Fig. 1 since only one spectral channel was positioned and there is no associated H_2O maser.

Table 3 lists the amplitude, velocity and position of each OH and H_2O maser with spectral channel amplitude greater than 0.3 Jy in each field. The position of the peak of the 23 GHz continuum emission is also listed if detected. The complete database contains over 1900 lines and is therefore only available electronically. However, a representative field (351.42+0.64) is printed here as an example. The HII and maser positions are given as offsets in arc seconds relative to the reference position listed in Table 2. Note that the offsets are in celestial coordinates, so a $+1''$ offset in RA and Dec moves the maser spot to the left (east) and up (north) on the sky. The velocity is the center velocity of the VLA channel map imaged. No attempt at fitting velocities of individual spectral features was made.

Spectra and positions for the OH and H_2O masers in each field are plotted in Fig. 1. There are a total of 74 spot maps in the complete figure, which is only available in electronic form. An example for the field 351.42+0.64 (NGC6334N) is printed here as Fig. 1. The source name is given at the top left of the sky plot, and the OH and H_2Obeam sizes are shown schematically to the right (OH beam cross-hashed). Note that the beams are not to scale, but have the correct position angle and aspect ratio. Table 2 should be consulted for the size of the beams in arc seconds. Linear size scales are given to the right of each sky plot, with the near and far distances (if ambiguous) printed at the top of each scale. The symbols in the sky plot are crosses (×) for OH and circles (◯) for H_2O. The corresponding grayed symbols represent the *mean* position of the maser spots for that species (note that the grayed crosses become gray squares). The grayed symbols do not necessarily correspond to an actual maser position. The star symbol, if present, represents the position of the continuum peak detected at 23 GHz.

Below the sky plots are the OH and H_2O maser spectra measured at the VLA. The two maser species are plotted on the same velocity scale, and the scale for each field spans a fixed range of 80 km s^{-1} for ease of comparison. Each spectrum has one filled (darker) symbol denoting the *median* velocity of each species. For fields in which only one species was detected, only one spectrum is shown.

Below the spectra are listed the following values derived from the spot maps. If no continuum source or only one maser species was detected some items are not

displayed. Linear sizes in mpc are given for both near and far distances.

1. The *total extent* (in arcsec, mpc and km s^{-1}) of the OH and H_2O masers in the field.
2. The *separation* of the *mean* positions and the *median* velocity of the OH and H_2O masers in the field.
3. The *separation* between the position of the *peak* continuum emission and the *mean* positions of the OH and H_2O masers in the field.

Several minor modifications have been made to the original FC89 database. First, the assumed distance has been revised from 2.0 to 5.7 kpc for 9.62+0.20 (Hofner et al. 1994). Second, deep imaging of the continuum emission at 9 GHz has been obtained for fields between 353° and 25° galactic longitude (Forster & Caswell, in preparation). The new observations show that three of the 23 GHz continuum detections listed in FC89 (359.14+0.03, 359.62–0.25, and 12.91–0.26) are spurious. These have therefore been removed from the FC89 database. In addition, new observations of OH and H_2O masers and H II regions toward some of the fields in FC89 have provided independent measurements of the absolute positions. These are discussed in the next section. Finally, a misprint in FC89 for the reference position of the OH maser 11.90–0.14 has been corrected.

3. Discussion

FC89 estimated the absolute position errors in the database at ∼0.″5 rms for both OH and H_2O maser reference features. The registration between the two species therefore has an uncertainty of ∼0.″7 rms. Comparison of the 23 GHz continuum peaks with 2 cm VLA images for 351.42+0.64 (Rodriguez et al. 1982) and 10.62–0.38 (Ho & Haschick 1981) indicated offsets in position of ∼1″. FC89 also noted that comparisons with previously published positions of seven OH masers and continuum sources from Garay et al. (1985) and Gaume & Mutel (1987) gave a maximum difference of ∼2″, with most <1″, consistent with an rms error of ∼0.″5. However, for more southerly declinations, especially south of −35°, there may be somewhat larger errors. In particular, Caswell et al. (1995) remark that the OH FC89 position for 339.88–1.26 appears to be too far north by 4″. Similarly, for 347.63+0.15, Caswell (1997) suggests that the OH position as measured by FC89 may be too far north by 3″.

Hofner & Churchwell (1996) published positions and spectra for 21 H_2O masers associated with UCH II regions, eight of which overlap with FC89. Comparison of the maser positions for these eight sources gives a mean offset of 0.″85. By far the largest discrepancy (2.″48) was found for 34.26+0.15. Omitting this source gives a mean offset of 0.″64. This is the quadratic sum of the error in the two datasets, and is in agreement with an rms error ∼0.″5 for the FC89 data. We want to emphasize that in comparing the location of the masers in the FC89 database with other sources the uncertainty in absolute position must be taken into account.

Another important consideration is the size and orientation of the synthesized beam. The position of each H_2O maser spot listed in Table 3 and plotted in Fig. 1 has been derived from a parabolic fit to the corresponding VLA channel map (the AIPS task MAXFIT). For the OH masers a Gaussian fit was used (the MAD equivalent of the AIPS task IMFIT). For a point source such a fit gives positions whose accuracy is determined by the signal-to-noise ratio and the size of the synthesized beam. For a signal-to-noise ratio of 10 the fits give positions accurate to ∼0.″2 rms for a beamsize of 5″. This means that the *relative* positions of maser spots of the same species brighter than 1 Jy are determined to < 0.″3 rms for for a 5″ beam. For weak maser features the elongation of the synthesized beam may produce linear structure which is not real. Possible examples of this effect are the sources 341.22–0.21 and 347.63+0.15. One should therefore beware of apparent linear structure on scales <1″ which has the same orientation as the synthesized beam.

A related problem arises if several maser features with overlapping velocities but different positions are present. Owing to the simple fitting procedures used to derive the maser positions, beam blending can cause systematic spatial and kinematical effects which may not be real. A possible example is 351.42+0.64 (NGC 6334F). The H_2O masers in this source appear as many spots in a string ∼2″ long, offset ∼3″ north of a compact cluster of masers near the reference position (see Fig. 1). The H_2O beam has a fwhm size of 2.″0 by 1.″3. Table 3 lists the spectrum and locations of the maser spots for this source, showing that several H_2O maser spots with the same velocity occur at different positions. Maser spots with the same velocity appear together in a single VLA channel map, and are therefore blended to some extent by convolution with the synthesized beam.

In 351.42+0.64 several spots in the compact group of H_2O masers near the reference position have small northern offsets. These spots have the same velocity as the strongest masers in the string, so it is possible that these small offsets are caused by beam blending. Likewise, the string itself may actually contain only 2 or 3 discrete groups with overlapping velocity ranges, which are blended in the VLA observations to appear as an almost continuous string. This ambiguity can only be resolved by new observations at higher resolution. The overall extent and general distribution of masers should not be seriously affected by beam blending. However, the effects of beam blending should be considered when interpreting apparent systematic spatial-velocity structure in these sources.

4. Summary

The OH and H_2O masers observed at the VLA by FC89 represent a large sample of massive star-forming regions containing both maser species in the galaxy. The masers are often associated with ultra-compact HII regions, dense molecular cores, FIR objects and molecular outflows. The relationship between the masers and these other objects, and with the massive stars which are the presumed energy source for the masers, remains an active area of research. Until this relationship is better understood, the promise of these bright molecular-line sources to probe the environment of massive star-forming complexes will not be fulfilled.

We have provided in electronic form the complete VLA database of interstellar OH and H_2O masers analyzed by FC89. Maps, spectra and beams are shown for all 74 fields observed. Several changes to the original database, and some caveats to its use for spatial and kinematical analysis were discussed. The database will be useful in interpreting continuum and molecular line observations of star-forming regions, for investigating the spatial and kinematical relation between the masers and their local environment, and in studies of the spatial and temporal evolution of the OH and H_2O masers themselves.

Acknowledgements. We gratefully acknowledge the help of Shane Ebersole in preparing the figures for publication.

References

Caswell J.L., 1998, MNRAS 297, 215
Caswell J.L., 1997, MNRAS 289, 203
Caswell J.L., Vaile R.A., Forster J.R., 1995, MNRAS 277, 210
Codella C., Testi L., Cesaroni R., 1997, A&A 325, 282
Carral P., Kurtz S.E., Rodriguez L.F., De Pree C., Hofner P., 1997, ApJ 486, L103
Ellingsen S.P., Norris R.P., McCulloch P.M., 1996, MNRAS 279, 101
Forster J.R., Caswell J.L., 1989, A&A 213, 339 (FC89)
Ho P.T.P., Haschick A.D., 1981, ApJ 248, 622
Hofner P., Kurtz S., Churchwell E., Walmsley C.M., Cesaroni R., 1994, ApJ 429, L85
Hofner P., Churchwell E., 1996, A&AS 120, 283
Kraemer K.E., Jackson J.M., 1995, ApJ 439, L9
Garay G., Reid M.J., Moran J.M., 1985, ApJ 289, 681
Gaume R.A., Mutel R.L., 1987, ApJS 65, 193
Rodriguez L.F., Canto J., Moran J.M., 1982, ApJ 255, 103

Table 2. FC89 database - reference positions

Source	B1950		J2000		Distance		OH Beam			H_2OBeam		
Gal Coords	RA(h m s)	Dec(° ′ ″)	RA(h m s)	Dec(° ′ ″)	near (kpc)	far	size″		PA°	size″		PA°
339.68-1.21	16 47 26.00	-46 11 02.4	16 51 06.23	-46 16 06.8	2.4	(16.4)				6.0	1.4	-1
339.88-1.26	16 48 24.60	-46 03 34.7	16 52 04.63	-46 08 35.1	3.1	(15.7)	8.0	1.9	-2	5.7	1.4	0
340.06-0.24	16 44 35.93	-45 16 23.3	16 48 13.82	-45 21 39.6	4.6	14.2	8.0	1.9	-2	5.2	1.4	-3
341.22-0.21	16 48 41.65	-44 21 53.9	16 52 17.89	-44 26 53.2	(3.6)	15.3	7.2	1.6	0	4.8	1.4	3
343.13-0.06	16 54 44.03	-42 47 36.6	16 58 17.39	-42 52 10.7	3.2	15.9	5.2	2.2	30	4.4	1.4	1
344.23-0.57	17 00 35.15	-42 14 29.7	17 04 07.77	-42 18 39.1	3.4	15.8	4.4	2.7	-15			
344.58-0.02	16 59 26.43	-41 37 36.8	17 02 57.72	-41 41 51.1	0.7	18.6	4.7	1.5	-10	3.4	1.4	-11
345.00-0.22	17 01 40.14	-41 24 58.5	17 05 11.14	-41 29 03.4	3.2	16.1	5.6	1.4	5	3.8	1.4	40
345.01+1.79	16 53 17.28	-40 09 23.2	16 56 45.26	-40 14 03.6	3.0	(16.4)	4.8	1.9	35	3.5	1.3	6
345.41-0.95	17 06 02.18	-41 32 06.3	17 09 33.68	-41 35 52.6	2.3	(17.1)	5.3	1.8	33	3.8	1.6	6
345.51+0.35	17 00 53.55	-40 40 18.5	17 04 23.02	-40 44 26.7	2.1	17.3	4.3	1.5	-10	2.8	1.4	-15
345.70-0.09	17 03 21.03	-40 47 00.0	17 06 50.87	-40 50 57.8	1.0	18.4	5.9	1.7	36	3.2	1.3	11
347.63+0.15	17 08 24.22	-39 05 49.0	17 11 51.07	-39 09 25.4	9.7		6.0	1.7	35			
348.55-0.98	17 15 53.37	-39 00 49.9	17 19 20.41	-39 03 54.2	2.5	(17.1)	5.2	1.5	8			
348.70-1.04	17 16 39.83	-38 54 13.6	17 20 06.69	-38 57 14.6	1.8	(17.8)	4.7	2.4	-42	2.2	1.3	-23
348.89+0.10	17 12 24.93	-38 06 52.7	17 15 50.13	-38 10 12.0	8.9	10.7	5.6	1.6	15			
348.89-0.18	17 13 34.67	-38 16 14.5	17 17 00.21	-38 19 28.8	1.0	21.1	4.5	1.2	19	4.2	1.2	-25
349.07-0.02	17 13 25.55	-38 01 58.8	17 16 50.65	-38 05 13.7	1.0	23.2	5.5	1.4	15	3.5	1.4	13
349.09+0.11	17 12 59.62	-37 56 30.6	17 16 24.53	-37 59 47.4	9.8		6.4	1.7	35	2.4	1.3	18
350.02+0.43	17 14 22.13	-37 00 03.2	17 17 45.39	-37 03 14.2	5.0	14.7	6.1	1.7	38	2.2	1.3	21
350.11+0.09	17 16 01.18	-37 07 17.7	17 19 24.72	-37 10 21.5	9.8		4.6	1.2	-21	4.4	1.4	-31
351.16+0.70	17 16 36.08	-35 54 51.0	17 19 57.50	-35 57 52.4	1.7	(18.1)	4.8	1.5	20	2.4	1.8	18
351.42+0.64	17 17 32.34	-35 44 02.5	17 20 53.48	-35 46 59.9	1.9	(17.9)	6.4	1.5	39	2.0	1.3	24
351.58-0.35	17 22 03.27	-36 10 05.5	17 25 25.33	-36 12 43.4	9.9		4.5	1.7	20	2.3	1.3	20
351.78-0.54	17 23 20.32	-36 06 44.0	17 26 42.32	-36 09 16.3	2.2	17.6	4.7	2.2	-52	2.0	1.3	-23
352.52-0.15	17 23 50.87	-35 17 00.9	17 27 11.43	-35 19 31.1	8.0	11.8	4.7	1.6	23	2.1	1.4	24
353.41-0.36	17 27 05.56	-34 39 21.7	17 30 25.14	-34 41 37.9	4.5	15.3	5.9	1.5	46	1.9	1.3	26
353.46+0.56	17 23 33.02	-34 05 54.6	17 26 51.55	-34 08 26.2	8.4	11.4	5.0	1.3	25	3.4	1.2	28
354.61+0.47	17 26 59.99	-33 11 38.2	17 30 17.11	-33 13 54.9	4.2	15.7	5.0	1.3	30	1.5	1.1	29
355.34+0.15	17 30 12.54	-32 45 56.6	17 33 29.03	-32 47 59.4	2.0	(20.0)	7.7	1.1	44	1.7	1.2	29
358.23+0.11	17 37 41.46	-30 21 08.6	17 40 54.23	-30 22 39.0	10.0		5.9	1.5	-46	1.3	1.2	-39
359.14+0.03	17 40 13.96	-29 37 57.9	17 43 25.65	-29 39 17.2	5.0	15.0	4.3	1.2	30	1.4	1.1	30
359.44-0.10	17 41 28.68	-29 26 59.8	17 44 40.10	-29 28 13.7	10.0		5.8	1.4	48	1.5	1.2	32
359.62-0.25	17 42 27.70	-29 22 21.2	17 45 39.01	-29 23 30.8	10.0		4.5	1.2	30	1.3	1.0	33
359.97-0.46	17 44 09.22	-29 10 57.7	17 47 20.26	-29 12 00.0	10.0		7.3	1.1	46	1.5	1.2	34
0.38+0.04	17 43 11.23	-28 34 34.0	17 46 21.34	-28 35 40.5	10.0		5.2	1.0	35	1.3	1.0	34
0.55-0.85	17 47 03.83	-28 53 39.5	17 50 14.45	-28 54 29.1	2.0	18.0	5.1	1.3	40	1.2	1.0	36
2.14+0.01	17 47 28.19	-27 04 59.2	17 50 36.11	-27 05 47.1	8.9	11.1	5.8	0.9	40	1.1	1.0	38
3.91+0.00	17 51 33.02	-25 34 14.5	17 54 38.76	-25 34 44.6	5.8	14.2	5.0	1.4	-60			
5.88-0.39	17 57 26.83	-24 03 56.5	18 00 30.45	-24 04 00.9	2.6		6.2	1.3	51	1.3	1.2	37
8.67-0.36	18 03 18.75	-21 37 53.4	18 06 19.02	-21 37 32.3	5.8	14.0	6.2	1.2	52	1.2	1.2	40
8.68-0.37	18 03 23.23	-21 37 31.1	18 06 23.49	-21 37 09.7	5.8	14.0	6.2	1.2	52			
9.62+0.20	18 03 15.99	-20 31 54.9	18 06 14.79	-20 31 34.0	5.7		4.8	1.1	40	1.1	1.0	40
10.62-0.38	18 07 30.56	-19 56 28.8	18 10 28.56	-19 55 49.4	6.0		6.0	1.2	50	1.2	1.1	42
11.03+0.06	18 06 42.56	-19 21 56.0	18 09 39.81	-19 21 20.2	3.2	16.0	4.9	1.2	40	1.1	1.0	38
11.90-0.14	18 09 15.09	-18 42 16.5	18 12 11.46	-18 41 29.6	5.1	14.4	6.4	1.1	51			
12.22-0.12	18 09 43.81	-18 25 05.7	18 12 39.81	-18 24 16.7	(3.4)	16.1	5.1	1.3	40	1.0	1.0	43
12.68-0.18	18 10 59.17	-18 02 42.5	18 13 54.68	-18 01 48.0	6.4	(13.1)	7.5	1.0	52	3.0	2.8	46
12.91-0.26	18 11 44.18	-17 52 57.8	18 14 39.47	-17 52 00.1	4.4	(15.1)	5.4	1.3	45	1.0	1.0	45
14.17-0.06	18 13 32.25	-16 41 01.7	18 16 26.00	-16 39 56.2	5.0	14.4				3.2	2.4	-48
15.03-0.68	18 17 29.91	-16 13 11.0	18 20 23.05	-16 11 48.2	2.5	(16.7)	3.8	1.7	-53	4.1	2.2	-51
16.59-0.05	18 18 18.05	-14 33 14.7	18 21 09.10	-14 31 48.5	5.6	13.6	7.2	1.0	53	2.8	2.3	48
19.61-0.13	18 24 29.05	-11 55 34.0	18 27 16.84	-11 53 41.1	4.7							
19.61-0.23	18 24 50.25	-11 58 31.7	18 27 38.09	-11 56 37.2	3.8	(14.6)	4.7	1.2	50	3.1	2.7	46
23.01-0.41	18 31 56.10	-09 03 03.7	18 34 40.39	-09 00 38.5	(5.6)	12.8	6.5	1.0	-59	3.9	1.8	-54
23.44-0.18	18 31 55.53	-08 34 03.9	18 34 39.25	-08 31 38.8	7.8	10.5	4.8	1.1	45	3.0	2.3	47
24.79+0.08	18 33 30.43	-07 14 43.2	18 36 12.58	-07 12 11.3	7.7	10.4	4.7	1.2	-63	4.2	1.7	-55
28.86+0.07	18 41 08.28	-03 38 34.5	18 43 46.22	-03 35 29.8	8.5		5.5	1.2	57	2.2	1.6	53
31.21-0.18	18 46 20.91	-01 40 10.3	18 48 56.57	-01 36 43.4			6.5	1.1	56	2.3	1.5	54
31.24-0.11	18 46 09.49	-01 36 38.8	18 48 45.08	-01 33 12.7	1.6	15.5	6.1	1.4	56	2.5	1.6	54
31.28+0.06	18 45 36.44	-01 30 02.2	18 48 11.91	-01 26 38.5	8.5		6.2	1.3	55	2.8	1.6	54
32.74-0.07	18 48 47.81	-00 15 43.5	18 51 21.86	-00 12 06.2	2.5	14.3	4.1	1.4	53	2.6	1.8	50
33.13-0.09	18 49 34.25	00 04 32.2	18 52 07.91	00 08 12.7	5.6	11.1	7.0	1.0	55	2.9	1.6	55
34.26+0.15	18 50 46.36	01 11 13.9	18 53 18.76	01 14 59.5	4.2	(12.3)	6.2	1.0	55	3.1	1.6	55
35.03+0.35	18 51 29.12	01 57 30.7	18 54 00.64	02 01 19.3	3.0	13.3	4.0	1.2	46	2.6	1.8	57
35.20-0.74	18 55 41.05	01 36 31.1	18 58 12.98	01 40 37.5	2.3	14.0	4.4	0.9	48	3.3	1.6	55
35.20-1.74	18 59 13.24	01 09 13.5	19 01 45.68	01 13 34.9	2.9	(13.4)	7.2	1.0	56	2.9	1.7	52
35.58-0.03	18 53 51.38	02 16 29.4	18 56 22.55	02 20 28.1	3.5	(12.8)	4.7	1.1	45	3.2	1.8	52
40.62-0.14	19 03 35.43	06 41 57.2	19 06 01.63	06 46 36.8	2.3	12.9	3.9	1.2	45	2.8	1.1	55
43.80-0.13	19 09 30.98	09 30 46.8	19 11 54.05	09 35 51.1	(2.6)	11.8	7.0	1.0	58	2.9	1.4	57
45.07+0.13	19 11 00.40	10 45 43.1	19 13 22.06	10 50 53.5	(4.3)	10.0	4.4	1.3	40	2.9	1.6	54
45.47+0.05	19 12 04.42	11 04 11.0	19 14 25.75	11 09 25.8	(5.4)	8.6	3.6	1.1	44	3.5	1.1	54
45.47+0.13	19 11 45.97	11 07 02.9	19 14 07.24	11 12 16.5	(4.7)	9.3	8.0	1.2	54	3.0	1.4	57
48.61+0.02	19 18 12.93	13 49 44.7	19 20 31.19	13 55 24.8	(1.5)	11.8	8.0	1.0	56	3.1	1.4	58
49.49-0.39	19 21 26.30	14 24 41.8	19 23 43.96	14 30 35.1	(5.3)	7.7	4.5	1.0	-61	4.4	1.4	-58

Table 3. FC89 database (this is a sample only; the full table containing all sources is available electronically)

351.42+0.64	B1950: 17 17 32.34	−35 44 02.5		
	S(Jy)	Vel(km s^{-1})	RA(″)	Dec(″)
HII			0.10	−1.00
OH	1.95	−6.16	0.48	−0.07
	3.80	−6.71	0.30	0.30
	40.40	−7.26	0.10	0.50
	21.05	−7.81	0.12	0.48
	34.15	−8.35	−0.15	0.45
	135.25	−8.90	−0.20	0.40
	8.55	−9.45	−0.20	0.40
	1.80	−10.00	0.12	0.68
	1.80	−10.55	1.17	1.62
	4.45	−11.10	0.78	1.40
	5.40	−11.65	0.40	1.12
	1.80	−12.19	0.27	1.48
H_2O	3.30	−0.77	−0.29	3.06
	22.40	−2.09	−0.38	3.22
	24.70	−3.41	−0.51	3.96
	74.90	−4.73	−0.55	3.76
	75.80	−6.05	−0.55	4.19
	246.20	−7.36	−0.63	5.07
	227.60	−8.68	−0.68	4.84
	21.30	−8.68	0.11	0.52
	7.50	−10.00	0.17	0.58
	66.90	−10.00	−0.62	4.32
	37.60	−11.32	−0.52	4.03
	43.00	−12.64	−0.49	4.66
	2.60	−12.64	−0.16	0.04
	6.40	−13.95	0.00	0.20
	8.40	−13.95	−0.34	4.18
	6.10	−15.27	−0.30	3.25
	5.00	−15.27	0.01	0.05
	4.30	−16.59	−0.06	0.03
	8.20	−16.59	−0.30	3.26
	4.30	−17.91	−0.04	0.02
	2.40	−17.91	−0.32	3.26
	4.20	−19.23	−0.05	−0.03
	3.80	−20.54	−0.06	−0.01
	4.30	−21.86	−0.03	0.01
	4.20	−23.18	−0.04	0.01
	5.00	−25.82	−0.02	−0.01
	12.70	−27.13	−0.02	−0.01
	11.10	−28.45	−0.01	0.00
	45.10	−29.77	0.00	0.00
	69.30	−31.09	0.00	0.00
	22.30	−32.41	0.00	0.00
	1.80	−33.72	−0.02	0.02
	1.00	−35.04	0.02	0.03
	2.80	−36.36	−0.76	4.88
	1.60	−37.68	−0.75	5.01
	1.10	−41.63	−0.61	4.46
	1.60	−45.59	−0.32	3.53

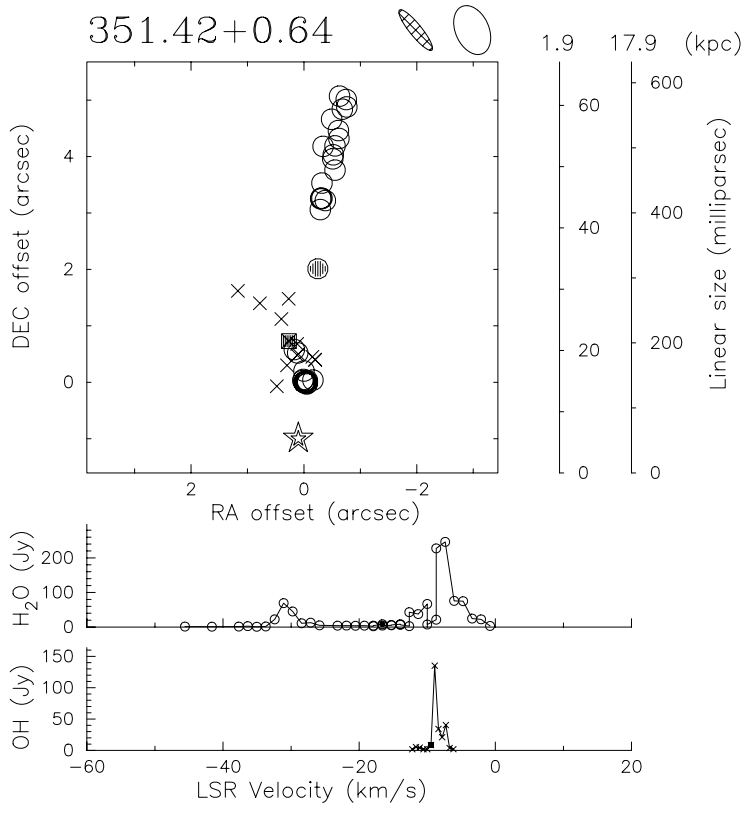

Extent	arcsec	. . . .mpc. . . .		Vel (km/s)
OH	1.8	17	159	6.0
H_2O	5.1	47	445	44.8
Separation				
OH−H_2O	1.4	13	120	7.1
HII−OH	1.7	16	151	
HII−H_2O	3.0	28	263	

Fig. 1. The locations of H_2O masers are indicated by circles and OH masers by crosses. The corresponding grayed symbols represent the mean position of the maser spots for that species and do not necessarily correspond to an actual maser position. The position of the peak of the 23 GHz continuum emission is indicated by a star symbol if detected. The synthesized beams are shown next to the source name. The beams (OH cross-hatched) have the correct position angle and aspect ratio, but are not to scale. Linear scale bars are given for both near and far distances (if ambiguous) with the preferred distance located nearest the spot map. OH and H_2O spectra are displayed below the maps. See the text for an explanation of the items listed below the spectra